

PACS numbers: 42.55.Rz; 42.60.Gd; 42.60.Fc
DOI: 10.1070/QE2015v045n06ABEH015604

On the possibility of a new passively *Q*-switched laser operation mode with periodic wavelength switching

A.V. Fedorov, A.A. Fomichev, M.E. Doroshenko

Abstract. **The possibility of cw-pumped passively *Q*-switched laser operation has been examined theoretically. Also, we have proposed laser operation mode in which the output wavelength automatically switches between two values without any changes in cavity parameters. Using numerical simulation and an Er:YAG laser with a Co:ZnSe passive *Q*-switch as an example, we have found parameters that ensure such operation mode.**

Keywords: *passive Q-switching, lasing, two-frequency laser system.*

1. Introduction

The study of chaotic and periodic lasing dynamics in passively *Q*-switched systems is of interest for both practical application and basic research of multidimensional dynamic systems [1]. Gaining insight into the dynamic behaviour of a laser system is necessary for understanding the processes that influence the noise characteristics of laser radiation and for the ability to produce systems with automatic and periodic modulation of output laser characteristics (wavelength, output energy and polarisation) [1–4]. Rate equations are effectively used in studies of spectral and frequency-domain collective phenomena in laser media, in particular in studies of antiphase dynamics and polarisation effects [5, 6].

Antiphase dynamics are usually investigated in systems with a passive *Q*-switch and are due to so-called spatial hole burning in the gain medium [4, 7]. The studies in question examined microchip lasers in which the output wavelength λ switched between several wavelengths spaced ~1 nm apart. Spatial hole burning in a gain element (GE) is most pronounced when its length meets the inequality $l_a < \lambda^2/\Delta\lambda \sim$ 1 mm, and the effect is strongest in microchip lasers, so the use of such lasers is usually limited to applications which employ laser systems with a low average output power. At the same time, some applications require high pulse energies and high average output powers.

In this paper, we propose a new mechanism based on the dependence of the laser wavelength on the inversion in a GE in a quasi-two-level system. In such lasers, pumping and emission take place between Stark components of the same multiplets of the GE. Such systems include diode-pumped Yb lasers operating on the $^2F_{5/2} \rightarrow {}^2F_{7/2}$ transition ($\lambda \sim 1030$ nm) [8]. Another frequently studied case is lasing on the Er^{3+} $^4I_{13/2} \rightarrow {}^4I_{15/2}$ transition [9] under optical pumping by InP laser diodes ($\lambda = 1.4-1.5$ μm) or an Er-doped fibre laser at a wavelength of 1.5 μm. Yet another frequently employed laser system is Ho^{3+} lasers operating on the $^5I_7 \rightarrow {}^5I_8$ transition, at a wavelength of ~2.1 μm. The most widespread optical pump source for this system is a Tm-doped fibre laser ($\lambda = 1.9$ μm) [9]. Owing to the small Stokes shift and the good overlap between the pump and laser emission spectra, the efficiency of these lasers may reach its theoretical maximum, exceeding 80% [10].

There are two key reasons for creating such laser systems. One reason is the conversion of the diode laser pump output with a relatively low brightness into a high-quality beam, as required for many practical applications. The other is the conversion of continuous pump radiation (from diode or fibre lasers) into pulsed radiation. *Q*-switched lasers may have high efficiency and operate at a high pulse repetition rate. Under cw pumping, such laser systems combine high average power (typical of cw lasers) with high peak power (characteristic of *Q*-switched pulsed modes).

One inherent feature of laser systems pumped on the same multiplet transition as is used for lasing is that their output wavelength depends on the inversion in the GE. The reason for this is that the lower laser level is partially populated at room temperature and because of this the effective gain cross section is determined by absorption and amplification processes [11].

This paper examines the possibility of producing cw-pumped *Q*-switched laser systems with an output wavelength λ periodically switching between λ_1 and λ_2 without changes in cavity parameters or pump intensity. Lasers based on such an effect might be potential candidates for applications in mechanical micromachining, remote sensing, range finding, microsurgery and contamination monitoring. They also might be of interest for lidar and other atmospheric studies where one has to periodically tune to and detune from absorption lines of particular gaseous species.

2. Effect of population inversion on the laser wavelength

Consider how a gain spectrum is influenced by inversion in the case of resonance excitation, as exemplified by Yb:YAG, Er:YAG and Ho:YAG crystals. Owing to the Boltzmann distribution at each laser multiplet, the spectral characteris-

A.V. Fedorov, A.A. Fomichev Moscow Institute of Physics and Technology (State University), Institutskii per. 9, 141700 Dolgoprudnyi, Moscow region, Russia;
e-mail: anton.v.fedorov@hotmail.com;
M.E. Doroshenko A.M. Prokhorov General Physics Institute, Russian Academy of Sciences, ul. Vavilova 38, 119991 Moscow, Russia

Received 29 June 2014; revision received 20 February 2015
Kvantovaya Elektronika **45** (6) 515–520 (2015)
Translated by O.M. Tsarev

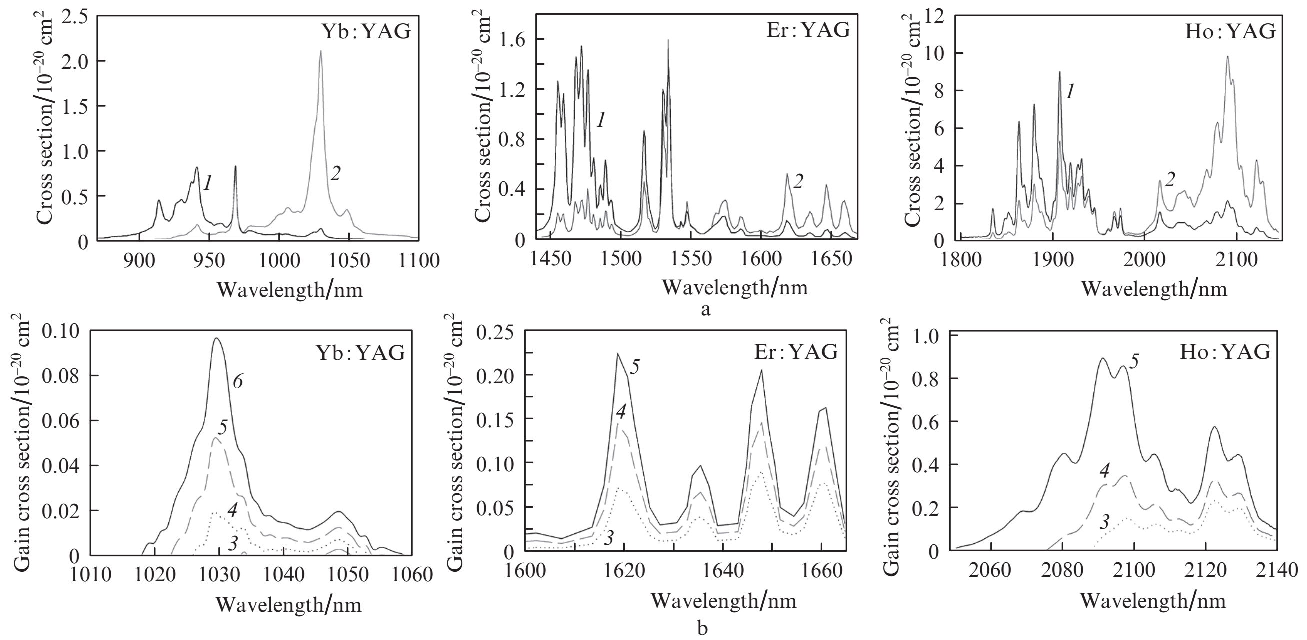

Figure 1. (a) (*1*) Absorption and (*2*) luminescence cross section spectra of Yb:YAG, Er:YAG and Ho:YAG crystals; (b) gain cross section spectra of Yb:YAG GEs at n_2 = (*3*) 0.053, (*4*) 0.065, (*5*) 0.08 and (*6*) 0.1, Er:YAG GEs at n_2 = (*3*) 0.32, (*4*) 0.437 and (*5*) 0.45 and Ho:YAG GEs at n_2 = (*3*) 0.18, (*4*) 0.20 and (*5*) 0.25.

Table 1. Spectroscopic parameters of laser transitions.

Parameter	Yb:YAG		Er:YAG		Ho:YAG	
	λ_1 (1030 nm)	λ_2 (1049 nm)	λ_1 (1617 nm)	λ_2 (1645 nm)	λ_1 (2090 nm)	λ_2 (2121 nm)
$\sigma_e/10^{-20}$ cm^2	2.11	0.34	0.52	0.43	0.981	0.427
$\sigma_a/10^{-20}$ cm^2	0.13	0.02	0.14	0.07	0.17	0.13
$\xi_0 = \sigma_a/(\sigma_e+\sigma_a)$	0.06	0.05	0.21	0.14	0.17	0.13
n_{cr}	0.06		0.44		0.20	

tics of a laser medium can be characterised by the total population of each multiplet and the spectral dependences of the absorption and gain cross sections [9, 11–15]. Figure 1a presents the absorption cross section $\sigma_a(\lambda)$ and luminescence cross section $\sigma_e(\lambda)$ spectra of these crystals. It is worth pointing out that $\sigma_e(\lambda) \neq \sigma_a(\lambda)$ as a result of the averaging over transitions between individual components, and the total gain and absorption in the medium are determined by the interplay between these processes. Denoting the relative excited state population by $n_2 = N_2/N_0$ (where N_2 is the average excited state concentration and N_0 is the total laser centre concentration in the GE), we introduce the gain cross section $\sigma_g(\lambda, n_2)$ following Setzler et al. [11]:

$$\sigma_g(\lambda, n_2) = [n_2\sigma_e(\lambda) + (n_2 - 1)\sigma_a(\lambda)]. \quad (1)$$

Figure 1b shows calculated gain cross section spectra of Yb:YAG, Er:YAG and Ho:YAG crystals at various inversions in GEs. Consider the spectra in greater detail, using an Er:YAG crystal as an example. It is seen that, at low inversions [curves (*3*)], the maximum gain is reached at λ = 1645 nm. At the same time, with increasing inversion [curve (*4*)] the cross section at λ = 1617 nm rises most rapidly, and at $n_2 \sim 0.437$ the cross sections at these wavelengths become equal to each other. At higher inversions, the maximum gain is observed at λ = 1617 nm [curve (*5*)]. Similarly, the peak gain wavelength changes in Ho:YAG (from 2121 to 2090 nm) and Yb:YAG (from 1049 to 1030 nm) crystals.

The inversion (n_2) at which the gain cross sections at two wavelengths become equal to each other will be referred to as critical (n_{cr}). It is clear from Fig. 1 that, to ensure periodic laser wavelength switching between 1645 and 1617 nm, it is necessary that, at instants when the lasing threshold is reached, the inversion be alternately above and below the critical level. The critical inversion depends on the relationship between the gain and luminescence cross sections at the two wavelengths:

$$n_{cr} = \frac{\sigma_a(\lambda_1) - \sigma_a(\lambda_2)}{[\sigma_e(\lambda_1) + \sigma_a(\lambda_1)] - [\sigma_e(\lambda_2) + \sigma_a(\lambda_2)]}. \quad (2)$$

The spectroscopic parameters of the above laser transitions are listed in Table 1.

3. Model for laser operation

To analyse the operation of a passively Q-switched laser, we use the point model, which has been effectively used since the 1960s for describing cw and Q-switched laser operation [6].

This model can be represented by the following system of linear differential equations:

$$\begin{cases} \dot{N}_2 = I_p(\sigma_{ap}N_1 - \sigma_{ep}N_2) + I_{01}(\sigma_{a01}N_1 - \sigma_{e01}N_2) \\ \quad + I_{02}(\sigma_{a01}N_1 - \sigma_{e02}N_2) - \dfrac{N_2}{\tau_n}, \\ \dot{M}_2 = \sigma_{am}(M_0 - M_2)(I_{01} + I_{02})\left(\dfrac{S_a}{S_m}\right) - \dfrac{M_2}{\tau_m}, \\ \dot{I}_{01} = \dfrac{I_{01}}{t_{rt}}[(\sigma_{e01}N_2 - \sigma_{a02}N_1)2l_n - 2M_1 l_m \sigma_{am} - L_{cav}], \\ \dot{I}_{02} = \dfrac{I_{02}}{t_{rt}}[(\sigma_{e02}N_2 - \sigma_{a02}N_1)2l_n - 2M_1 l_m \sigma_{am} - L_{cav}]. \end{cases} \quad (3)$$

Here, I_0 and I_p are the average lasing and pump photon flux densities in the GE, respectively; N_1 and N_2 are the average ground and excited state concentrations in the GE, respectively; N_0 is the total laser centre concentration in the GE; M_1 and M_2 are the average concentrations in the passive Q-switch in the ground and excited states, respectively; and $M_0 = M_1 + M_2$ is the total concentration.

The first equation describes the variation of the inversion in the GE. The first term on the right-hand side of this equation describes excitation and stimulated de-excitation processes under the action of pumping (σ_{ap} and σ_{ep} are the absorption and luminescence cross sections at the pump wavelength, respectively). The second and third terms represent analogous processes under the action of light of intensities I_{01} and I_{02} at the laser wavelengths λ_1 and λ_2 ($\sigma_{a0(1,2)}$ and $\sigma_{e0(1,2)}$ are the absorption and luminescence cross sections at the laser wavelengths). The last term on the right-hand side of the equation under consideration describes excited state relaxation processes with an excited state lifetime τ_n.

The second equation describes analogous processes in the passive Q-switch. Here, σ_{am} is the absorption cross section in the passive Q-switch at the laser wavelength (the same at λ_1 and λ_2) and τ_m is the excited state lifetime in the passive Q-switch. In the model under consideration, we excluded the effect of pump radiation on the processes in the passive Q-switch and neglected the light amplification processes in it.

The last two equations describe the intracavity lasing intensity dynamics. Here, t_{rt} is the cavity round-trip time; l_n is the GE length; l_m is the length of the passive Q-switch; $L_{cav} = -\ln(R) + \gamma_p$ is the total loss in the cavity (the same at λ_1 and λ_2); R is the reflectivity of the output coupler of the cavity; and γ_p is the logarithmic decrement for the single-pass passive loss in the cavity. To find the exact solution to the equations in question, numerical calculation is needed, but many important features of laser operation, critical for the ability to ensure periodic laser wavelength switching, can be inferred from qualitative analysis of the behaviour of the system.

4. Inversion build-up in the cavity to the threshold level

A cw-pumped passively Q-switched laser generates repetitive pulses. Consider the period of population inversion build-up after generation of a laser pulse ($t = 0$). The pulse leads to a drop in inversion in the GE to some minimum level, $N_{2min} \neq 0$, and causes bleaching of the passive Q-switch ($M_2 = 1$). After that, pumping increases the inversion from N_{2min} to the threshold value n_{2th}, where the next laser pulse begins. Throughout this process, we have $I_{01}, I_{02} = 0$, so the first equation in (3) has no terms containing laser beam intensity. The solution to this equation has the form

$$n_2 = \left(\frac{j_p}{j_p + 1}\xi_p\right) \times \left\{1 - \left[1 - \frac{n_{2min}}{[j_p/(j_p+1)]\xi_p}\right]\exp\left(-t\frac{j_p + 1}{\tau_n}\right)\right\}. \quad (4)$$

Here, $j_p = I_p/(\sigma_a + \sigma_{ep})\tau_n$ is the dimensionless pump intensity and $\xi_p = \sigma_{ap}/(\sigma_{ap} + \sigma_{ep})$ is a spectroscopic parameter determining the relationship between the absorption and luminescence cross sections at the pump wavelength. In Fig. 2, lines (*1*) and (*2*) represent the pumping-induced population inversion build-up (at $j_p = 5$ and $\xi_p = 1$) at different initial n_{2min} values.

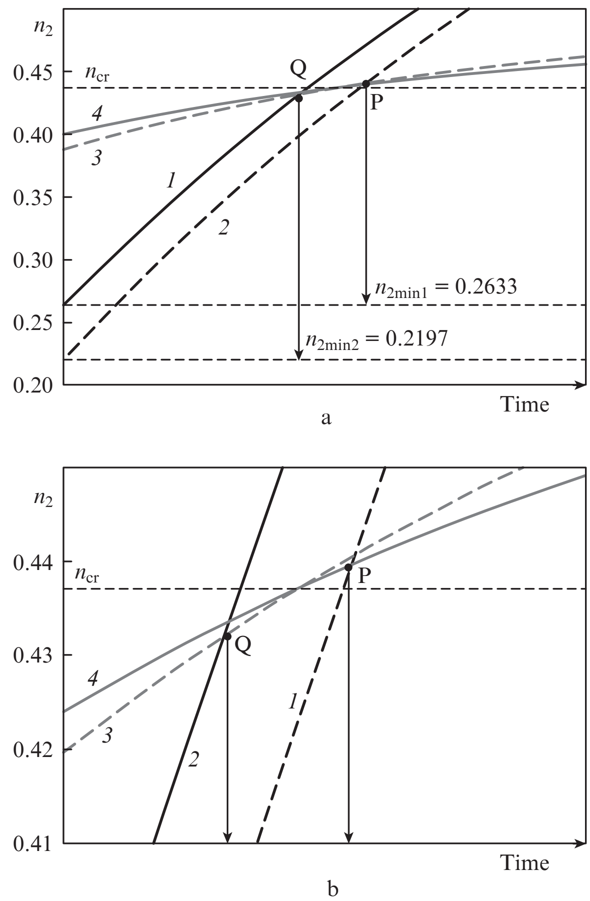

Figure 2. (a) (*1*, *2*) Time dependences of the inversion in a GE and (*3*, *4*) threshold inversions at λ_1 and λ_2, respectively; (b) threshold inversion region on expanded scales.

The inversion in the GE increases until it reaches the threshold value, where lasing begins. The threshold inversion n_{2th} in the GE is determined by the condition that the round-trip gain at the laser wavelength be equal to the total loss in the cavity. From the third and fourth equations in (3), this condition can be represented in the form

$$n_{2th} = \xi_0\left[1 - \frac{L_{cav} - 2\ln(T_m)(1 - m_2)}{2\ln(T_0)}\right]. \quad (5)$$

Here, $T_m = \exp(-\sigma_{am}l_m M_0)$ is the initial transmission of the passive Q-switch at the laser wavelength; $m_2 = M_2/M_0$ is the relative concentration of active centres in an excited state in the passive Q-switch; and $\xi_0 = \sigma_{a0}/(\sigma_{a0} + \sigma_{e0})$ and $T_0 = \exp(-N_0\sigma_{a0}l_n)$ are spectroscopic characteristics of the GE at the laser wavelength.

After the laser pulse, the inversion in the passive Q-switch (m_2) decays as an exponential function of time, which can be derived from the second equation in (3):

$$m_2 = \exp(-t/\tau_m). \qquad (6)$$

The time dependences of the threshold inversion in the system at λ_1 and λ_2 are shown in Fig. 2 by lines (*3*) and (*4*). In our calculations, we used spectroscopic parameters of an Er:YAG GE ($\xi_{01} = 0.21$, $\xi_{02} = 0.14$) and Co:ZnSe passive Q-switch. The initial transmission of pulses was taken to be $T_{02} = 0.75$, with an initial transmission of the Q-switch $T_m = 0.8$ and R = 55%. It is seen in Fig. 2 that, at threshold inversions $n_{2th} < n_{cr} = 0.437$, threshold will be reached at the wavelength λ_2; for $n_{2th} > n_{cr}$, the threshold level will be reached at λ_1. Moreover, it is seen in Fig. 2 that, when the inversion increases from its minimum value n_{2min2}, the threshold level will be reached at the laser wavelength λ_1 (point P), whereas when the inversion increases from its minimum value n_{2min1}, threshold will be reached at λ_2 (point Q). The cavity loss and pump intensity are the same in both cases.

It follows from the above analysis that, to ensure lasing with automatic wavelength switching between λ_1 and λ_2, cavity parameters should be adjusted so that, as a result of lasing at λ_2, the inversion will decrease from point P to n_{2min1}, whereas lasing at λ_1 will cause the inversion to decrease from point Q to n_{2min2}.

5. Numerical simulation of repetitive pulse generation

As a model for numerical simulation, we considered an Er:YAG laser operating at λ_1 = 1617 nm and λ_2 = 1645 nm. In our computations, the length of the Er:YAG crystal was 3 cm and the erbium content was 0.655 at %. A Co:ZnSe crystal with an initial transmittance of 85% was used as a passive Q-switch. The ratio of the laser mode area in the GE to the mode area in the passive Q-switch was 10. The cavity length was 15 cm and the reflectivity of the output coupler was R = 57% at both laser wavelengths. The laser was cw-pumped at λ_p = 1.46 μm and an intensity I_p = 7.2 kW cm^{-2}. In the numerical simulation, we used the free software environment R.

The simulation results indicate that, at the above parameters, the system operates at two wavelengths, independent of the initial values of n_2 and m_2. As seen in Fig. 3a, local maxima in population inversion alternate from pulse to pulse, one of the maximum values being above n_{cr}, and the other, below. As a result, the laser wavelength switches between λ_1 = 1617 nm and λ_2 = 1645 nm (Figs 3b, 3c). Figure 3d illustrates the population inversion dynamics in the passive Q-switch. The pulse spacings T_1 and T_2 are 0.33 and 0.44 ms, and the average repetition rate is 2.6 kHz. The ratio of the maximum intensities at the two wavelengths is 0.77.

The range of cavity losses where two-wavelength lasing is observed (for the initial transmission of the passive Q-switch fixed at T_m = 85%) is shown in Fig. 4 [curve (*1*)] and corresponds to the maximum threshold loss in the cavity at a given pump intensity. In the region above curve (*1*), the cavity loss

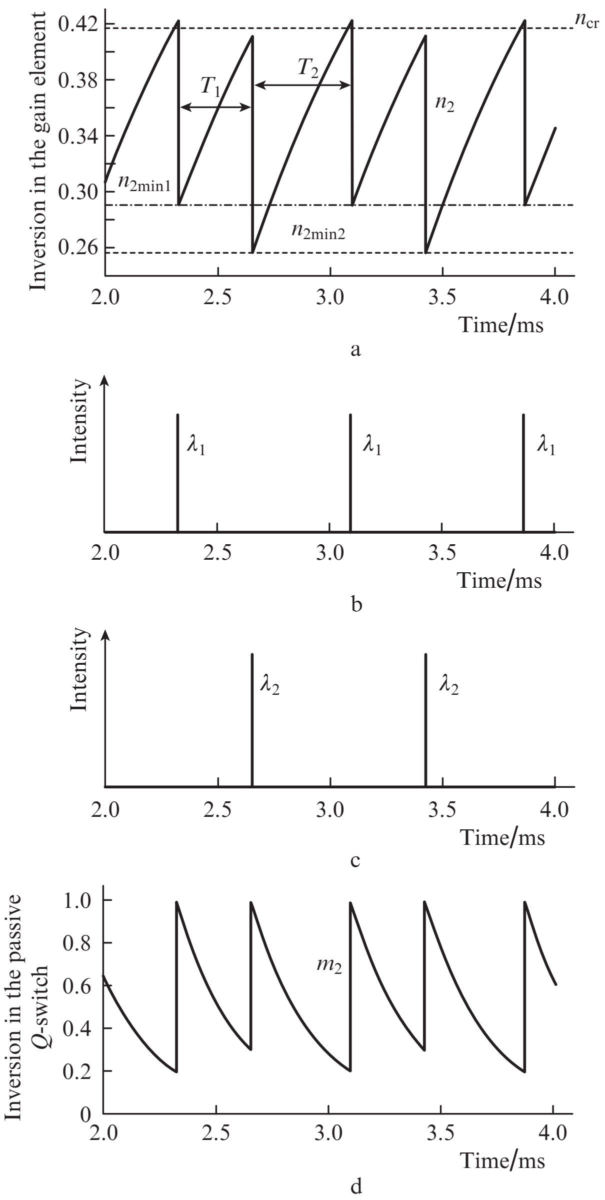

Figure 3. Lasing with switching between two wavelengths after every laser pulse: (a) inversion dynamics in the GE, (b, c) laser pulse intensity at λ_1 = 1617 nm and λ_2 = 1645 nm, respectively, and (d) inversion dynamics in the passive Q-switch.

parameters and pump intensity are such that lasing is impossible (the loss is too high). In the region between curves (*1*) and (*2*), the laser emits at the wavelength λ_1. The region under curve (*5*) corresponds to such cavity loss parameters and pump intensities at which the laser operates at the wavelength λ_2.

The wavelength switching regime takes place between curves (*3*) and (*4*) (Fig. 4, inset). The transition from lasing at the wavelength λ_1 [the region between curves (*1*) and (*2*)] or λ_2 [the region under curve (*5*)] to that with wavelength switching between λ_1 and λ_2 [the region between curves (*3*) and (*4*)] includes regions [between curves (*2*) and (*3*) or (*4*) and (*5*)] where wavelength switching also occurs, but the switching period exceeds two pulse spacings. Such operation mode is exemplified in Fig. 5. It is seen that a periodic sequence of three pulses is generated (one pulse at the wavelength λ_1 and two at λ_2).

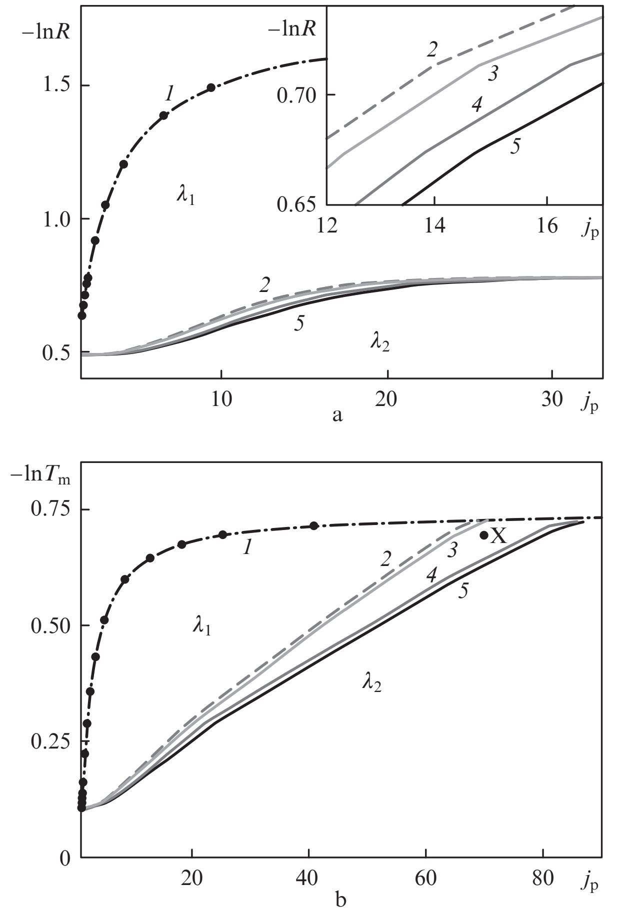

Figure 4. (a) Regions of permissible pump parameters (j_p) and active losses ($-\ln R$) at which lasing with wavelength switching between λ_1 and λ_2 takes place (inset: region with j_p = 14–16 on expanded scales); (b) regions of permissible j_p values and initial transmission values of the passive *Q*-switch ($-\ln T_m$) at which the above lasing mode takes place at R = 55%. Point X corresponds to j_p = 70 and T_m = 50%.

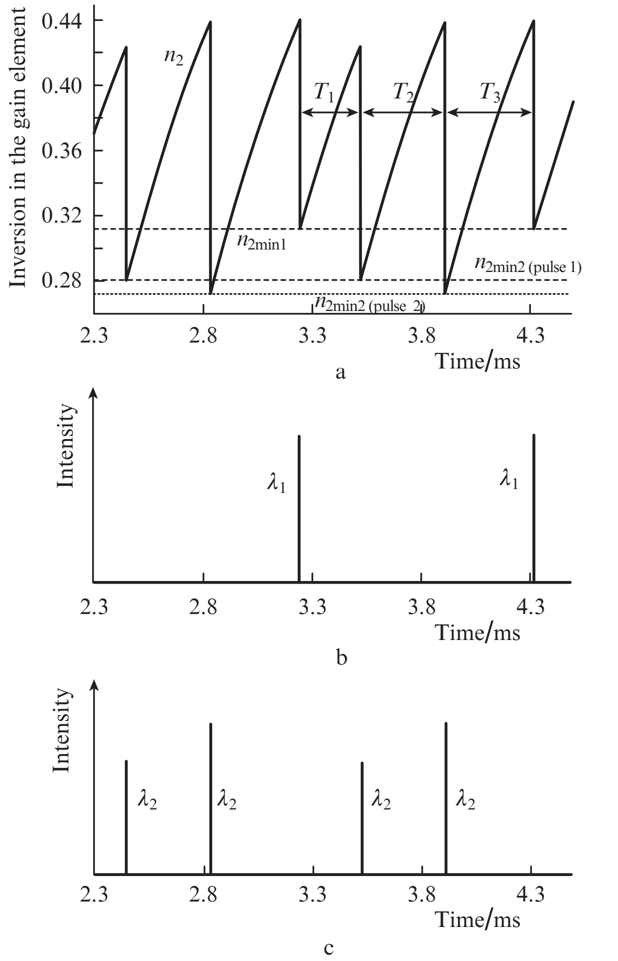

Figure 5. Lasing with wavelength switching between λ_1 and λ_2 at a switching period equal to three pulse spacings: (a) inversion dynamics in the GE; (b, c) intensities of laser pulses at λ_1 = 1617 nm and λ_2 = 1645 nm, respectively.

It follows from Fig. 4a that the region where wavelength switching is possible is rather large: limited by reflectivities R from 46% to 61% and pump intensities I_p from 4 to 27 kW cm^{-2}. In the example represented in Fig. 5, the permissible change in pump intensity is ~12% (at R = 57%) and the permissible change in cavity loss is 4% (at I_p = 7.2 kW cm^{-2}).

Consider also the effect of the initial transmission of the passive *Q*-switch (at a constant cavity loss R = 55%). Figure 4b shows the analytically (*1*) and numerically (points) obtained threshold transmission as a function of the dimensionless pump intensity j_p. It is seen that the minimum initial transmission of the passive *Q*-switch is $\ln T_m$ = 0.73, or T_m ~ 48%. Curves (*1*)–(*5*) in Fig. 4b are the boundaries of the same regions as in Fig. 4a. At the same time, in contrast to that in Fig. 4a, the region corresponding to lasing with wavelength switching [between curves (*3*) and (*4*)] is limited to initial transmittances in the range T_m = 48%–88% and pump intensities I_p = 4–72 kW cm^{-2}. The maximum permissible change in pump intensity at point X is ~18% (at T_m = 50%) and the permissible change in cavity loss at this point is ~7% (at I_p = 63 kW cm^{-2}). The region of parameters around point X is of interest for obtaining lasing with periodic wavelength switching because there is either no lasing (the loss is too high) or lasing with periodic wavelength switching.

6. Conclusions

We have examined the possibility of a new passively *Q*-switched, cw-pumped laser operation mode. Numerical simulation results suggest that, in this laser operation mode, the output wavelength will automatically switch between two wavelengths after every pulse, without changes in cavity parameters. Using an Er:YAG laser with a Co:ZnSe passive *Q*-switch as an example, we have found parameters that ensure such operation mode. At a cavity length of 15 cm, GE length of 3 cm, Er content of 0.655 at%, 85% initial transmittance of the passive *Q*-switch, ratio of the mode area in the GE to the laser mode area in the passive *Q*-switch of 10 and reflectivity of the output coupler R = 57%, this operation mode takes place at λ = 1.46 μm and pump intensity I_p = 7.2 kW cm^{-2}. The permissible change in each parameter (pump intensity, reflectivity of the output coupler and initial transmission of the passive *Q*-switch), at which wavelength switching persists, is 12%.

References

1. Liu Y., Oliveira P.C., Danailov M.B., Rios Leite J.R. *Phys. Rev. A*, **50**, 3464 (1994).
2. Park J.-D., McKay A., Dawes J.M. *Opt. Express*, **17**, 6053 (2009).

3. Dong J., Ueda K., Yang P. *Opt. Express*, **17**, 16980 (2009).
4. Dong J., Li J., Huang S., Shirakawa A., Ueda K. *Opt. Commun.*, **256**, 158 (2005).
5. Shahruz S.M. *Phys. D: Nonlin. Phenom.*, **142**, 291 (2000).
6. Siegman A.E. *Lasers* (Sausalito, Cal: Univ. Sci. Books, 1986) p. 1283.
7. Dong J., Shirakawa A., Ueda K. *Laser Phys. Lett.*, **4**, 109 (2007).
8. Taira T., Tulloch W.M., Byer R.L. *Appl. Opt.*, **36**, 1867 (1997).
9. Payne S.A., Chase L.L., Smith L.K., Kway W.L., Krupke W.F. *IEEE J. Quantum Electron.*, **28**, 2619 (1992).
10. Shen D.Y., Sahu J.K., Clarkson W.A. *Opt. Lett.*, **31**, 754 (2006).
11. Setzler S.D., Francis M.P., Young Y.E., Konves J.R., Chicklis E.P. *IEEE J. Sel. Top. Quantum Electron.*, **11**, 645 (2005).
12. Beach R.J. *IEEE J. Quantum Electron.*, **31**, 1606 (1995).
13. Nabors C.D. *IEEE J. Quantum Electron.*, **30**, 2896 (1994).
14. Fan T.Y. *IEEE J. Quantum Electron.*, **28**, 2692 (1992).
15. Beil K., Fredrich-Thornton Susanne T., Tellkamp F., Peters R., Kränkel C., Petermann K., Huber G. *Opt. Express*, **18**, 20712 (2010).